SCALE SEPARATION FOR IMPLICIT LARGE EDDY SIMULATION

X.Y. Hu
Lehrstuhl für Aerodynamik
Technische Universität München
Ad85748 Garching, Germany
xiangyu.hu@aer.mw.tum.de

N. A. Adams
Lehrstuhl für Aerodynamik
Technische Universität München
Ad85748 Garching, Germany
nikolaus.adams@tum.de

ABSTRACT

With implicit large-eddy simulation (ILES) the truncation error of the discretization scheme acts as subgrid-scale (SGS) model for the computation of turbulent flows. Although ILES is comparably simple, numerical robust and easy to implement, a considerable challenge is the design of numerical discretization schemes resulting in a physically consistent SGS model. In this work, we consider the implicit SGS model of the adaptive central-upwind weighted-essentially-non-oscillatory scheme (WENO-CU6) (*Hu, XY, Wang, Q. & Adams, NA, J. Comput. Phys., 229 (2010) 8952-8965.*) by incorporating a physically-motivated scale-separation formulation. Scale separation is accomplished by a simple modification of the WENO weights. The resulting modified scheme maintains the shock-capturing capabilities of the original WENO-CU6 scheme while it is also able to reproduce the Kolmogorov range of the kinetic-energy spectrum for turbulence at the limit of infinite Reynolds number independently of grid resolution. For quasi-isentropic compressible turbulence the the pseudo-sound regime of the dilatational kinetic-energy spectrum and the non-Gaussian probability-density function of the longitudinal velocity derivative are reproduced.

Introduction

Unlike standard large eddy simulation (LES) (for a review of LES for incompressible and compressible turbulence refer e.g. to (Sagaut 2006, Garnier et al. 2009), implicit LES (ILES) does not require an explicitly computed sub-grid scale (SGS) closure, but rather employs an inherent, usually nonlinear, regularization mechanism due to the nonlinear truncation error of the convective-flux discretization scheme as implicit SGS model. As finite-volume discretizations imply a top-hat filtered solution, regularized finite-volume reconstruction schemes were among the first ILES approaches, such as the flux-corrected transport (FCT) method (Boris et al. 1992), the piecewise parabolic method (PPM) (Colella et al. 1984). Although ILES is attractive due to its relative simplicity, numerical robustness and easy implementation, it often exhibits inferior performance to explicit LES (Garnier et al. 1999) if the discretization scheme is not constructed properly. Some schemes, such as PPM, FCT, MUSCL (Kim et al. 2005) and WENO (Balsara et al. 2000) methods, work reasonably well for ILES by being able to recover a Kolmogorov-range for high-Reynolds-number turbulence up to $k_{max}/2$, where k_{max} is the Nyquist wavenumber of the underlying grid (Grinstein et al. 2006, Grinstein et al. 2007, Thornber et al. 2007). These promising results have led to further efforts on the physically-consistent design of discretization schemes for ILES. Physical consistency implies the correct and resolution-independent reproduction of the subgrid-scale (SGS) energy transfer mechanism of isotropic turbulence. Based on this notion the adaptive local deconvolution method (ALDM) has been developed (Adams at al. 2004, Hickel et al. 2006) and successfully applied to a wide range of incompressible turbulent flows, e.g. Meyer et al. (2010) and Hickel et al. (2007). Approaches for decreasing excessive model dissipation for the solenoidal velocity field include the low-Mach number switch of Thornber et al. (2008), and the dilatation switch and shock sensor of Kawai et al. (2010).

In this work we propose a simple modification of an existing high-order WENO scheme which leads to a physically consistent implicit SGS model while preserving the shock-capturing properties of the underlying WENO scheme. Basis of this ILES scheme is a scale separation built into the nonlinear WENO weights that allows to differentiate between stencils providing contributions from resolved scales and from non-resolved scales. It avoids the need for explicit discretization-scheme switches (hybrid schemes) or flow sensors and operates directly on the reconstruction or deconvolution procedure. We point out that physical consistency is recovered for both, the solenoidal and the dilatational components of the velocity field, without requiring an explicit differ-

entiation between these components.

Scale-separation method

For presentation of the scale-separation method we consider for simplicity a generic one-dimensional convective equation

$$\frac{\partial u}{\partial t} + \frac{\partial f(u)}{\partial x} = 0. \tag{1}$$

By applying a top-hat filter around $x_i = i\Delta x$, where i is an integer and Δx is the support of the filter G_i, i.e., $\overline{u}_i = G_i * u = \int_{x_i-\Delta x/2}^{x_i+\Delta x/2} u(x)dx$, we obtain

$$\frac{\partial \overline{u}_i}{\partial t} + G_i * \frac{\partial f(u)}{\partial x} = \frac{\partial \overline{u}_i}{\partial t} + \frac{1}{\Delta x}\left(f_{i+1/2} - f_{i-1/2}\right) = 0, \tag{2}$$

where $f_{i\pm1/2} = f(u_{i\pm1/2})$ are the unknown exact fluxes at $x_i \pm \Delta x/2$. This is equivalent to taking a volume average over a computational cell as in a finite-volume discretization. Eq. (2) closed by replacing the exact fluxes by the numerical fluxes $\hat{f}^{k,r}_{i\pm1/2}$ at the cell faces

$$\frac{\partial \overline{u}_i}{\partial t} + \frac{1}{\Delta x}\left(\hat{f}^{k,r}_{i+1/2} - \hat{f}^{k,r}_{i-1/2}\right) = 0\,. \tag{3}$$

A consistent numerical flux is the cell-face value of a polynomial $\hat{f}^{k,r}_i(x)$ reconstructed from neighboring cell averages $\overline{f}_{i-k+r+1}, \ldots \overline{f}_i, \ldots, \overline{f}_{i+r}$, where k is the order of reconstruction. We consider the 6th-order non-dissipative symmetric reconstruction $\hat{f}^{6,3}_i(x)$ and the four admissible upwind- and downwind-biased 3rd-order reconstructions $\hat{f}^{3,r}_i(x)$, $r = 0,1,2,3$, which are dissipative or anti-dissipative. A physically consistent numerical flux is obtained by a proper weighting of these contributions, measured by local smoothness of the solution. In order to decrease the excess dissipation observed for the original WENO schemes the contribution of the higher order non-dissipative reconstruction should be emphasized for stencils containing resolved scales while dissipative reconstructions should be emphasized for stencils containing non-resolved scales. For this purpose the weighting strategy of the underlying WENO scheme needs to be modified.

We start from a variant of the original WENO scheme (Jiang et al. 1996), the adaptive central-upwind WENO scheme (WENO-CU6) (Hu et al. 2010). The adaptation between the higher order non-dissipative and lower order dissipative reconstructions requires the smoothness indicators

$$\beta^k_r = \sum_{n=1}^{k-1} \Delta x^{2n-1} \int_{x_i-\Delta x/2}^{x_i+\Delta x/2} \left(\frac{d^n}{dx}\hat{f}^{k,r}_i(x)\right)^2 dx \tag{4}$$

and a nonlinear weighting

$$\omega_r = \frac{\alpha_r}{\sum_{r=0}^{3}\alpha_r}, \quad \alpha_r = d_r\left(C + \frac{\tau^6}{\beta^3_r + \varepsilon}\right), \tag{5}$$

where d_r are linear weights which combine $\hat{f}^{3,r}_i(x)$, $r = 0,1,2,3$ to $\hat{f}^{6,3}_i(x)$. $C \gg 1$ is a positive parameter, ε is a small positive number, and τ^6 is a linear combination of β^6_3 and β^3_r, $r = 0,1,2$. Note that it is set $\beta^3_3 = \beta^6_3$ to assure that $\hat{f}^{3,3}_i(x)$ contributes only to the numerical flux of $\hat{f}^{6,3}_i(x)$. Although the WENO-CU6 exhibits much less numerical dissipation than classical WENO schemes, it still is too dissipative for physically consistent ILES (Hu et al. 2010).

While terms $\tau^6/(\beta^3_r + \varepsilon)$ are responsible for the WENO adaptation and give sufficient dissipation for flow discontinuities, the positive parameter C pushes the numerical flux to that of $\hat{f}^{6,3}_i(x)$ when the variation of $\tau^6/(\beta^3_r + \varepsilon)$ is relatively small. One could simply increase the value of C so that numerical dissipation is reduced for the resolved scales. However, this will lead to difficulties with the WENO adaptation for flow discontinuities and may result in numerical instability. Such an effect of inreasing C can be counterbalanced by steepening the $\tau^6/(\beta^3_r + \varepsilon)$ contribution in (5), leading to a stronger separation between resolved and non-resolved scales. For this purpose the following modified weighting, without deteriorating the order of accuracy of the original WENO-CU6 scheme, is introduced

$$\omega_r = \frac{\alpha_r}{\sum_{r=0}^{3}\alpha_r}, \quad \alpha_r = d_r\left(C_q + \frac{\tau^6}{\beta^3_r + \varepsilon}\right)^q, \tag{6}$$

where $C_q \gg C$ is a positive modeling parameter and $q > 1$ is an integer. Due to the power function the variation of $\tau^6/(\beta^3_r + \varepsilon)$ is strongly magnified. Note that this procedure operates on the reconstruction directly, and does not require a separation of solenoidal or compressional components of the velocity field. In particular, no explicit differentiation between shocks as subgrid scales and turbulent subgrid scales is needed.

Scale-separation method

Several test problems are provided to assess the potential of the scale-separation approach for ILES. Parameters are set to $C_q = 1000$ and $q = 4$ for all test problems. The flow is described by the compressible Navier-Stokes equation with the ideal-gas equation of state. As flows at very large Reynolds number are of interest physical viscosity is set to zero. The equation is solved by the above WENO methodology using an entropy-fix Roe numerical flux function (Jiang et al. 1996, Hu et al. 2010).

First we consider the three-dimensional Taylor-Green vortex to examine the capability of the ILES scheme to reproduce transition to turbulence. The initial flow field is given by

$$\begin{aligned} \rho &= 1, \\ (u,v,w) &= (\sin x \cos y \cos z, -\cos x \sin y \cos z, 0), \\ p &= 100 + \frac{1}{16}\left[(\cos 2x + \cos 2y)(2 + \cos 2z) - 2\right]. \end{aligned}$$

Final time of the computation is $t = 10$. The flow can be considered as incompressible since the pressure is chosen such

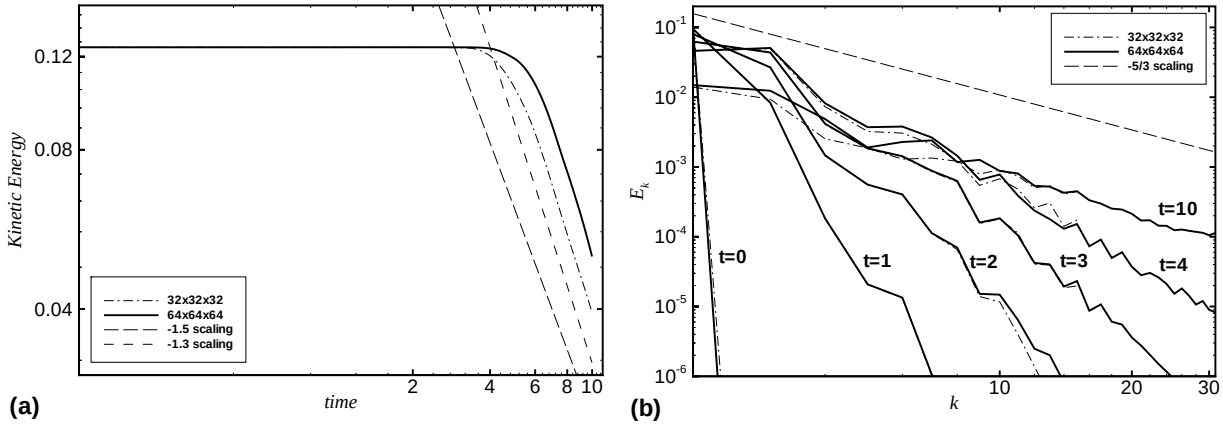

Figure 1. Taylor-Green Vortex: (a) evolution of kinetic energy; (b) energy spectrum at $t = 0$, 1, 2, 3, 4 and 10. The computations are performed on the periodic domain of $[0,0,0] \times [2\pi, 2\pi, 2\pi]$ on 32^3 and 64^3 grids.

that the Mach number becomes very small. The evolution of the kinetic energy and the energy spectrum at $t = 0, 1, 2, 4, 10$ are given in Fig. 1. As shown in Fig. 1a, at early stages kinetic energy is merely distributed among the resolved scales (total kinetic energy is constant). At about time $t = 4$ subgrid-scales are produced and kinetic energy begins to decay due to SGS dissipation, and eventually decays as $t^{-1.5}$, which is slightly faster than $t^{-1.2}$ found by Lesieur et al. (2003). A similar observation has been made for high-resolution ILES (Grinstein et al. 2006). Note also that experimental data indicate a rather large variation of the power-law exponent during different stages of decay, see Skrbek et al. (2000). As shown in Fig. 1b, the power-law kinetic-energy spectra clearly reflect the infinite-Reynolds-number limit, unlike that obtained by Cook (2007) with artificial-fluid LES at the same resolution, showing a pronounced artificial dissipative range. Between $t = 4$ and $t = 10$ turbulence develops, a the kinetic energy builds up a Kolmogorov intertial range, in agreement with the high-resolution LES of Grinstein et al. (2006). As the above behavior of our ILES scheme also is resolution independent, physical consistency is demonstrated by this test case.

Next we consider a shock density-wave interaction problem (Shu et al. 1989, Johnsen et al. 2010), which is an one-dimensional generic case to assess shock-capturing and wave-disturbance propagation capabilities of the model at the same time. The initial conditions are set by a Mach 3 shock interacting with a perturbed density field

$$(\rho, u, p) = \begin{cases} (3.857, 2.629, 10.333) & \text{if } 0 \le x < 1 \\ (1 + 0.2\sin(5x), 0, 1) & \text{if } 10 \ge x > 1 \end{cases}$$

and are evolved until final time $t = 1.8$. From the density, velocity and entropy profiles shown in Fig. 2, that the proposed ILES method not only captures the shock wave, but also maintains the amplitudes of density and entropy waves after passing through the shock with comparable or better accuracy than hybrid schemes (Johnsen et al. 2010, Adams et al. 1996). Note also that due to the lack of efficient scale separation the original WENO-CU6 exhibits larger artificial wave dissipation (Hu et al. 2010).

At last, we consider quasi-isotropic compressible turbulence at the limit of infinite Reynolds number with moderate initial Mach number. Both the solenoidal and dilatational velocity fields have relevant magnitude. For the dilatational field two distinguished regimes exist (Garnier et al. 2009): one is the the pseudo-sound regime where acoustic effects dominate; the other is the nonlinear subsonic regime where embedded weak shocks (shocklets) are generated. Initial velocity perturbations are introduced by randomly oriented, isentropic, sinusoidal sound and shear waves concentrated at the large scales with a root-mean-square (RMS) Mach number $\sqrt{3}u_{rms,0}/\langle c_0 \rangle = 0.5$. The initial data have a velocity power spectrum proportional to $k^4 \exp(-k^2/k_0^2)$, with $k_0 = 2$, and the ratio of compressible-component RMS to solenoidal-component RMS is $1/10$. Final time is $t = 6$ corresponding roughly to 6 turn-over times of the most energetic initial mode (Sytine et al. 2000). The solenoidal and dilatational spectra at $t = 1, 2, 4, 6$ are given in Fig. 3. A well-defined Kolmogorov-range up to wave number $k = 10$ has developed at $t = 2$, Fig. 3. This is in agreement with the simulation of Sytine et al. (2000)on a 256^3 grid. After $t = 4$ the Kolmogorov range extends up to k_{max}, independently of resolution, again indicating physical consistency of the model. As shown in Fig. 3b, the dilatational component develops in a different fashion. A Kolmogorov-range develops faster than for the solenoidal component for an intermediate wavenumber range. At larger wavenumbers a $-9/3$-range develops, which is in agreement with the theoretical predictions of the pseudo-sound regime (Garnier et al. 2009). A similar behavior is observed for the 32^3 grid, where the Kolmogorov-scaling is not that obvious, however. Another noteworthy observation for the solenoidal component is that a spectrum tail develops near k_{max}. After this tail has developed, it does not further steepen but rather decays self-similarly with the remainder of the spectrum. Such a behavior indicates that the spectrum tail is not a numerical artifact but at the high wave

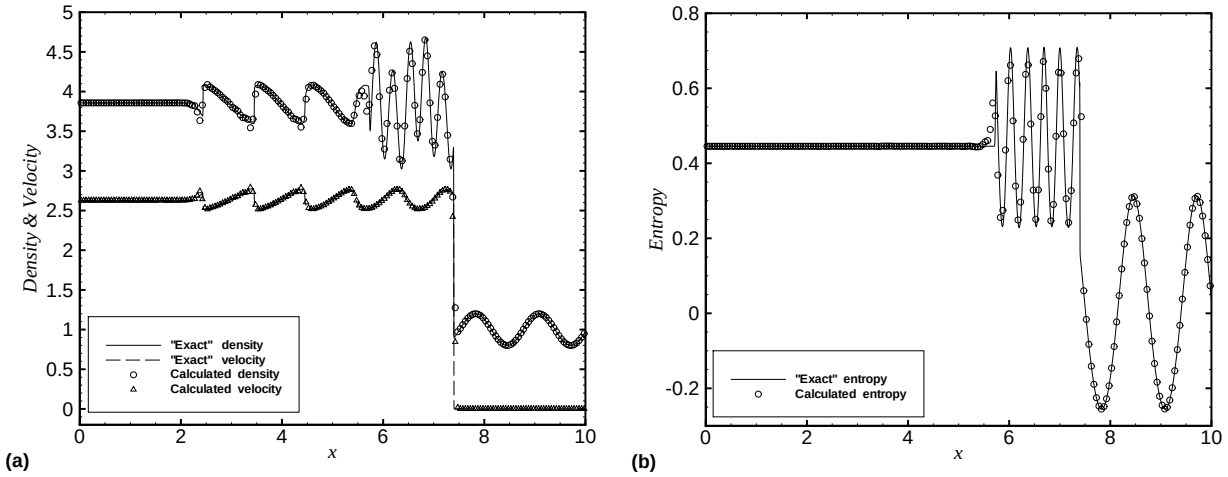

Figure 2. Shock density-wave interaction problem using a 200 points grid: (a) density and velocity profiles; (b) entropy profile. The "exact" solution is computed by the WENO-CU6 scheme with 3200 grid points.

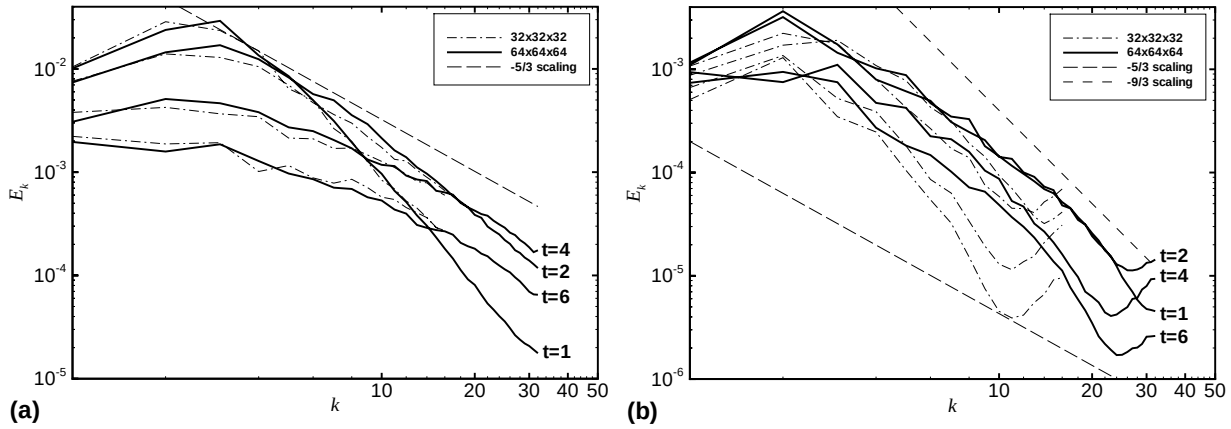

Figure 3. Energy spectrum at $t = 1$, 2, 4, 6 of a compressible quasi-isotropic turbulence with initial Mach number 0.5: (a) solenoidal spectra; (b) compressional spectra. The computations are performed on the periodic domain of $[0,0,0] \times [2\pi, 2\pi, 2\pi]$ on 32^3 and 64^3 grids.

number range. Although the energy increases with wave number along this tail, but rather has physical origin. A possible explanation is the occurence of shocklets where dilatational kinetic energy is concentrated. Evidence for shocklets is provided by contour plots of dilatation in Fig. 4a. Figure 4b shows the probability density function (PDF) of the longitudinal velocity derivative at $t = 4$, where the derivative u' is evaluated from a divided difference with the respective grid size. Whereas small velocity-derivative fluctuations follow a Gaussian PDF, large velocity-derivative fluctuations shows a distinct non-Gaussian, slightly skewed PDF, which is well established for isotropic turbulence. A quite good agreement with PDF from DNS for a similar setup but with Taylor-Reynolds number $Re_\lambda = 175$ (Samtaney et al. 2001) can be observed. Note that the present ILES gives a better agreement with DNS than some explicit LES simulations (Kang et al. 2003, Yakhot et al. 2005).

Concluding remarks

In this work we have proposed a scale separation approach for ILES. Scale separation is accomplished by a simple modification of the weighting strategy of an existing WENO scheme (WENO-CU6). Basic idea is to counterbalance a stronger bias towards the central high-order non-dissipative stencil by a higher integer power of the smoothness-measure contribution to the weights. This leads to a scale separation of contributions from resolved scales and non-resolved scales. Model parameters are the linear weight bias and the integer power exponent. It was shown that a straight-forward parameter choice is widely effective without further tuning. Numerical examples imply that the scale-separation WENO-

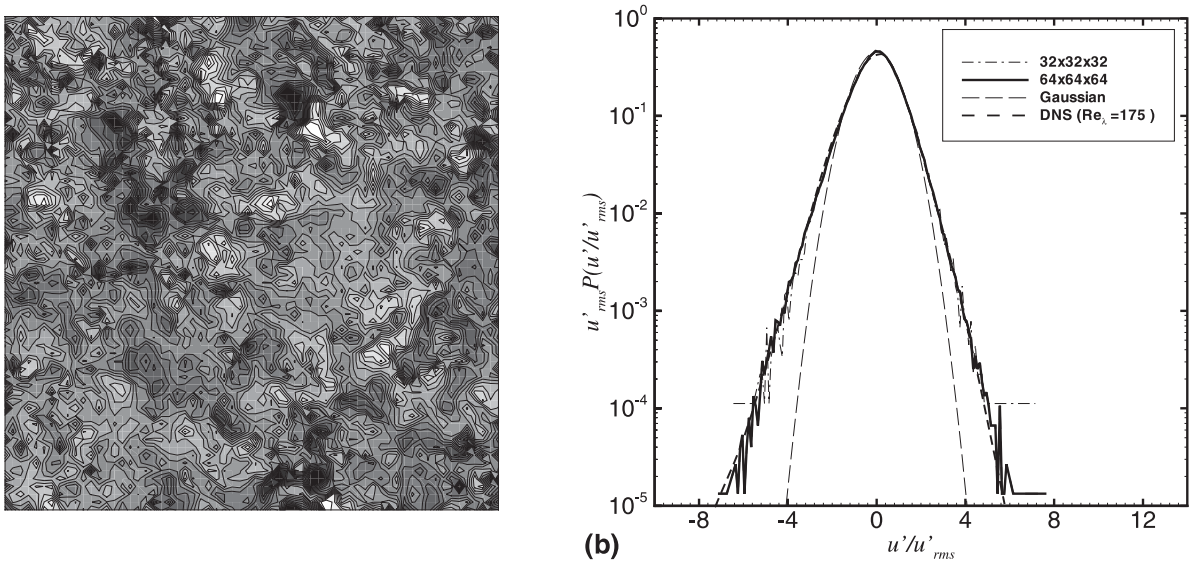

Figure 4. Compressible quasi-isotropic turbulence at time $t = 4$: (a) a slice of 15 dilatation contours from -2 to 2. Light and dark gray scales show positive and negative dilatation; (b) Longitudinal velocity derivative PDF with resolution. The refence DNS data is reproduced from Fig. 16 in Samtaney et al. (2001), where u' is evaluated with separation of $2\pi/64$.

CU6 scheme leads to a physically consistent implicit SGS model for incompressible and compressible turbulence, while the shock-capturing capabilities of the original WENO-CU6 scheme are maintained.

REFERENCES

NA Adams, S. Hickel, and S. Franz, 2004, "Implicit subgrid-scale modeling by adaptive deconvolution", J. Comput. Phys., Vol. 200, pp. 412-431.

N.A. Adams and Shariff K, 1996 "A high-resolution hybrid compact-ENO scheme for shock-turbulence interaction problems", J. Comput. Phys., Vol. 127, pp. 27-51.

D.S. Balsara and C.W. Shu, 2000, "Monotonicity preserving weighted essentially non-oscillatory schemes with increasingly high order of accuracy", J. Comput. Phys., Vol. 160, pp. 405-452.

J.P. Boris, F.F. Grinstein, E.S. Oran, and R.L. Kolbe, 1992, "New insights into large eddy simulation", Fluid dynamics research, Vol. 10, pp. 199-228.

P. Colella and P.R. Woodward, 1984, "The Piecewise Parabolic Method (PPM) for gas-dynamical simulations", J. Comput. Phys., Vol. 54, pp. 174-201.

A.W. Cook, 2007, "Artificial fluid properties for large-eddy simulation of compressible turbulent mixing", Physics of Fluids, Vol. 19, 055103.

E. Garnier, N.A. Adams, and P. Sagaut, 2009, "Large Eddy Simulation for Compressible Flows", Springer.

E. Garnier, M. Mossi, P. Sagaut, P. Comte, and M. Deville, 1999, "On the use of shock-capturing schemes for large-eddy simulation", J. Comput. Phys., Vol. 153, pp. 273–311.

F.F. Grinstein and C. Fureby, 2006, "Recent progress on flux-limiting based implicit Large Eddy Simulation," Proceedings, European Conference on Computational Fluid Dynamics, ECCOMAS CFD.

F.F. Grinstein, L.G. Margolin, and W. Rider, 2007, "Implicit large eddy simulation: computing turbulent fluid dynamics", Cambridge Univ Pr.

S. Hickel and N.A. Adams, 2007, "On implicit subgrid-scale modeling in wall-bounded flows", Phys. Fluids, Vol. 19, 105106.

S. Hickel, N.A. Adams, and J.A. Domaradzki, 2006 "An adaptive local deconvolution method for implicit LES", J. Comput. Phys., Vol. 213, pp. 413-436.

XY Hu, Q. Wang, and NA Adams, 2010, An adaptive central-upwind weighted essentially non-oscillatory scheme", J. Comput. Phys., Vol. 229, pp. 8952-8965.

G.S. Jiang and C.W. Shu, 1996, "Efficient implementation of weighted ENO schemes", J. Comput. Phys, Vol. 126, pp. 202–228.

E. Johnsen, J. Larsson, A.V. Bhagatwala, W.H. Cabot, P. Moin, B.J. Olson, P.S. Rawat, S.K. Shankar, B. Sjögreen, HC Yee, et al, 2010, "Assessment of high-resolution methods for numerical simulations of compressible turbulence with shock waves", J. Comput. Phys., Vol. 229, pp. 1213-1237.

H.S. Kang, S. Chester, and C. Meneveau, 2003, "Decaying turbulence in an active-grid-generated flow and comparisons with large-eddy simulation", Journal of Fluid Mechanics, Vol. 480, 129–160.

S. Kawai, S.K. Shankar, and S.K. Lele, 2010, "Assessment of localized artificial diffusivity scheme for large-eddy simulation of compressible turbulent flows", J. Comput. Phys., Vol. 229, pp. 1739-1762.

K.H. Kim and C. Kim, 2005, "Accurate, efficient and monotonic numerical methods for multi-dimensional compressible flows:: Part II: Multi-dimensional limiting process", Journal of computational physics, Vol. 208, pp. 570-615.

M. Lesieur and S. Ossia, 2000 "3D isotropic turbulence at very high Reynolds numbers: EDQNM study", Journal of Turbulence, Vol. 1, pp. 1-25.

M. Meyer, S. Hickel, and N.A. Adams, 2010, "'Assessment of Implicit Large-Eddy Simulation with a Conservative Immersed Interface Method for turbulent cylinder flow", Int. J. Heat Fluid Flow, Vol. 31, pp. 368-377.

P. Sagaut, 2006, "'Large eddy simulation for incompressible flows: an introduction", Springer Verlag.

P. Sagaut and C. Cambon, 2008, "'Homogeneous turbulence dynamics", Cambridge University Press.

R. Samtaney, DI Pullin, and B. Kosović, 2001, "Direct numerical simulation of decaying compressible turbulence and shocklet statistics", Physics of Fluids, Vol. 13, 1415.

C.W. Shu and S. Osher, 1989, "Efficient implementation of essentially non-oscillatory shock-capturing schemes", J. Comput. Phys., Vol. 83, pp. 32-78.

L. Skrbek and S.R. Stalp, 2000, "On the decay of homogeneous isotropic turbulence", Physics of fluids, Vol. 12, 1997.

I.V. Sytine, D.H. Porter, P.R. Woodward, S.W. Hodson, and K.H. Winkler, 2000, "Convergence tests for the piecewise parabolic method and Navier-Stokes solutions for homogeneous compressible turbulence", J. Comput. Phys., Vol. 158, pp. 225-238.

B. Thornber, A. Mosedale, and D. Drikakis, 2007, "On the implicit large eddy simulations of homogeneous decaying turbulence", J. Comput. Phys., Vol. 226, pp. 1902-1929.

B. Thornber, A. Mosedale, D. Drikakis, D. Youngs, and RJR Williams, 2008, "An improved reconstruction method for compressible flows with low Mach number features", J. Comput. Phys., Vol. 227, pp. 4873-4894.

V. Yakhot and K.R. Sreenivasan, 2005, "Anomalous scaling of structure functions and dynamic constraints on turbulence simulations", Journal of Statistical Physics, Vol. 121, pp. 823-841.